



HAL
open science

An improved thermal control of open cathode proton exchange membrane fuel cell

Chaima Mahjoubi, Jean-Christophe Olivier, Sondes Skander-Mustapha,
Mohamed Machmoum, Ilhem Slama-Belkhodja

► To cite this version:

Chaima Mahjoubi, Jean-Christophe Olivier, Sondes Skander-Mustapha, Mohamed Machmoum, Ilhem Slama-Belkhodja. An improved thermal control of open cathode proton exchange membrane fuel cell. International Journal of Hydrogen Energy, 2019, 44, pp.11332 - 11345. 10.1016/j.ijhydene.2018.11.055 . hal-03487004

HAL Id: hal-03487004

<https://hal.science/hal-03487004v1>

Submitted on 20 Dec 2021

HAL is a multi-disciplinary open access archive for the deposit and dissemination of scientific research documents, whether they are published or not. The documents may come from teaching and research institutions in France or abroad, or from public or private research centers.

L'archive ouverte pluridisciplinaire **HAL**, est destinée au dépôt et à la diffusion de documents scientifiques de niveau recherche, publiés ou non, émanant des établissements d'enseignement et de recherche français ou étrangers, des laboratoires publics ou privés.



Distributed under a Creative Commons Attribution - NonCommercial 4.0 International License

An improved thermal control of open cathode proton exchange membrane fuel cell

Chaima MAHJOUBI ^{1,2}, Jean-Christophe OLIVIER ², Sondes SKANDER-MUSTAPHA ^{1,3}, Mohamed MACHMOUM ²
and Ilhem SLAMA-BELKHODJA ¹

1. Université de Tunis El Manar, Ecole Nationale d'Ingenieurs de Tunis, LR11ES15 Laboratoire des Systèmes Electriques, 1002, Tunis, Tunisie.
2. Institut de Recherche en Énergie Électrique de Nantes-Atlantique IREENA (EA 4642), Université de Nantes, 37 Boulevard de l'Université, BP 406, 44602 Saint-Nazaire Cedex, France.
3. Université de Carthage, Ecole Nationale d'Architecture et d'Urbanisme, 2026, Sidi Bou Said, Tunisie

Abstract—Proton exchange membrane fuel cell is a well-known technology that has shown high efficiency and performance as a power system compared to conventional sources such as internal combustion engines. Especially, open cathode proton exchange membrane is growing more popular thanks to its simple structure, low cost and low parasitic losses. However, the open cathode fuel cell performance is highly related to the operating temperature variation and the airflow rate which is adjusted through the fan voltage. In this regard, the present study investigates the thermal management of an open cathode proton exchange membrane fuel cell. The objectives are the stack performance improvement and the stack degradation prevention. Indeed, a safety and optimal operating zone governed by the load current, the stack temperature and the air stoichiometry, is designed. This optimal operating zone is defined based on the system thermal balance and the operating constraints. Hence, the proposed control strategy deals concurrently with the stack temperature regulation and the air stoichiometry adjustment to guarantee the goals achievement. The performance of the proposed control strategy is verified through experimental studies with different operating conditions and results prove its efficiency. To properly design an appropriate control strategy, a multiphysic fuel cell model is developed based on acausal approach by mean of Matlab/Simscape and experimentally validated.

Keywords—Open cathod proton echange membrane fuel cell; control strategy; Fuel cell dynamique behaviour; airflow control; Stack temperature control; multiphysic model;

I. INTRODUCTION

PEM fuel cell system occupies over the last decades a central position as a clean energy conversion in a variety application such as automotive applications and renewable energy system [1][2][3][4] by generating electricity with water and heat production via chemical energy [5]. Nevertheless, water content in membrane and the stack operating temperature are considered as a vital factor which affect fuel cell performance and durability [6][7]. Therefore, water and thermal management are the two main issues to success the *PEM* fuel cell design and to improve its efficiency [8].

The *PEM* fuel cell system is a set of three subsystems, known as the balance of plant (*BOP*), consisting of the anode loop, the cathode loop and the cooling loop [9]. Generally, cooling subsystem consumes primary energy produced by the fuel cell and occupies space which leads to the stack efficiency decrease. Indeed, the cooling process energy consumption reaches around 4.6 % of the *PEM* fuel cell primary energy [10].

The open cathode *PEM* fuel cell mainly characterized by its cathode channels exposed to the ambient air. It is considered as an interesting system because of its simple structure, low cost and low parasitic losses [11]. In such

42 structure fans act to ensure the stack temperature regulation by forced convection and the reactant feeding (gas
43 stoichiometry) [12] [13]. Because there is an only actuator for functions already mentioned, a fine and adapted control
44 strategy is required to ensure the best balance and the best efficiency of the stack system, for a large range of operating
45 conditions, such as ambient temperature, relative humidity, load current and aging process.

46 Several research studies focus on the thermal management of closed or an open cathode fuel cell system based on only
47 one criterion. For example, in [14] the ancillary is controlled to carry out an optimal fuel cell temperature that
48 maximizes the output voltage. This temperature setting is modified with the stack current. A PID control is used to
49 control the cooling fan. The disadvantage of this method is that the fan control follows the dynamic of the temperature
50 (few minutes), while the air stoichiometric ratio has to be set at a much smaller time scale (few seconds). In [15] the
51 strong coupling between the optimal temperature control strategies, the stability and the efficiency of an open cathode
52 *PEM* fuel cell system is demonstrated. From a multi-physic and dynamical model, a control structure is proposed to
53 ensure the best efficiency and a sufficient stability. In this work, and unlike previous work [14], anticipation is added to
54 quickly reach the equilibrium point, regardless of the thermal time constant. In [16] the *PEM* fuel cell was adopted as a
55 power source for robots. To improve the operating conditions a fuzzy incremental *PID* control was developed to control
56 the temperature inside cells. The study's results show that the output power improvement is realized by the fitting
57 operating temperature at an optimal value.

58 Yet, not many research works focuses on thermal management of on open cathode fuel cell system based on more than
59 one criterion. In [17] an electrochemical and thermal model of an open cathode *PEM* fuel cell was developed combining
60 *PI* controller and the Extremum seeking controller in order to control the stack temperature, and by considering the air
61 stoichiometric ratio as a secondary parameter. However, this method seems efficient in steady state, especially around a
62 single operating point. In [18] a no dimensional flooding number is defined which is able to predict the best
63 stoichiometric ratio for different operating points . But, the optimal operating conditions obtained can be outside the
64 limits of thermal operation. Therefore, it is necessary in this case to degrade these optimal solutions to take the thermal
65 stresses into account. In [19] a multi-input multi-output fuzzy logic controller was performed in order to regulate stack
66 temperature and humidity simultaneously. The temperature regulation was based on the fan speed control considering
67 that the regulation with a criterion based on these two parameters permit to increase the stack performance. In [20] an
68 appropriate control strategy through oxygen mass flow rate regulation is achieved to avoid overheating and to
69 concurrently prevent air shortage of the open cathode fuel cell system. The airflow control is performed by selecting an
70 optimal oxygen excess ratio for both the power net improvement and the overheating protection. Experimental results
71 show that this control strategy improves the lifetime of the fuel cell system compared to other classical operating
72 schemes.

73 The present work takes into consideration concurrently two requirements to enhance the fuel cell performance which
74 are the temperature regulation and the air stoichiometric adjustment. Moreover, the axial fans are the only actuator for
75 the stack cooling by forced convection and the cathode air feeding. Thus, with such simple structure, it is more difficult
76 to carry out the control of these issues simultaneously. In this study, the axial fan voltage is regulated to specify the
77 stoichiometric ratio, which allows defining an optimal operating zone governed by three main parameters, which are the
78 stack temperature, the fan voltage and the load current. Two sets of operating constraints applied on both stack
79 temperature and fan operating voltage. By combining the thermal balance equation and the operating constraints, the
80 fuel cell optimal operating zone is defined guaranteeing the stack performance improvement and the stack degradation
81 prevention. In order to design a pertinent control strategy, a multi-physic fuel cell model is developed using

82 MATLAB/Simscape, to reproduce the stack dynamic behaviour at different operating conditions. An experimental
 83 study is carried out by a 2kW open cathode fuel cell system to valid the developed model and to evaluate the control
 84 strategy performance. This model will be very interesting to explore the proposed control strategy of the open cathode
 85 *PEM* fuel cell system. Thus, the challenge in this study is to guarantee the stack performance improvement and the
 86 stack degradation prevention while combining simultaneously both temperature regulation and air stoichiometric
 87 adjustment via fan voltage input. Hence, an optimal operating zone is defined in order to ensure the objectives
 88 achievement with respect to the thermal behavior of the open cathode *PEM* fuel cell and the environmental conditions
 89 variations (Ambient temperature).

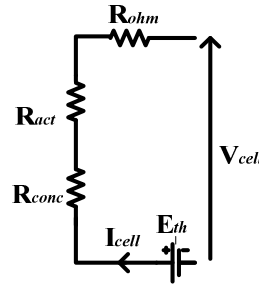
90 This study is organized as follows: the first section details the fuel cell models. The second section presents the
 91 experimental validation of the proposed model and its parameter estimations. The third part is dedicated for the
 92 proposed control strategy and its evaluation. The last part contains the conclusion.

93 II. FUEL CELL MODEL

94 In this section, a multi-physic fuel cell model is developed by taking into account different physical phenomena taking
 95 place within the stack. It offers the possibilities to design and test control strategies. In fact, an accurate and precise
 96 model is needed to emulate the *PEM* fuel cell dynamic behavior. So, two kinds of model are needed which are electrical
 97 and thermal ones.

98 A. Electrical fuel cell model

99 In literature, there are several equivalent circuit models of *PEM* fuel cell that describe its dynamic behavior. The
 100 adopted electrical model of the *PEM* fuel cell is presented in *Fig.1*.



101
 102 *Fig.1. Static electrical PEM fuel cell model*

103
 104 The adopted *PEM* fuel cell model is a static model using electrical circuits. It is composed of continuous voltage
 105 source E_{Nernst} associated with three resistors modeling the *PEM* fuel cell losses: activation losses, concentration losses
 106 and ohmic losses [25].

107 According to Nernst's equation (1), the cell potential depends on the temperature and reactants flow pressures (air
 108 and hydrogen). Decreasing the pressures of the reactants and / or increasing the temperature leads to the increase of the
 109 *PEM* fuel cell voltage output.

$$E_{Nernst} = E_0 + \frac{RT_{amb}}{2F} (\ln(P_{H_2}) + \frac{1}{2} \ln(P_{O_2})) \quad (1)$$

110 Where E_{Nernst} is the thermodynamic potential, E_0 reversible single cell potential, R is the molar gas constant, T_{amb} is
 111 ambient temperature, F is faraday constant, P_{O_2} and P_{H_2} are reactants pressure.

112 At standard conditions (P=1bar, T=25°C), the E_{Nernst} calculated value is based on either the high heating value *HHV*
 113 assuming the product water inside a fuel cell in the liquid phase, is approximately 1.48V. Or, it is based on the low
 114 heating value *LHV*, supposing the product water is in the gaseous phase, is about 1.25V [26]. Therefore, several cells
 115 are connected in series to be adapted for applications with high power. The *PEM* fuel cell output voltage V_{st} is given by
 116 the following equations:

$$V_{st} = NV_{cell} \quad (3)$$

117 Where N is the number of cells connected in series, V_{cell} is the output voltage of an elementary cell.

$$V_{cell} = E_{Nernst} - V_{act} - V_{ohm} - V_{conc} \quad (3)$$

118 Where V_{act} , V_{ohm} and V_{conc} are the voltage drop corresponding to activation loss, ohmic loss and concentration loss
 119 taking place inside the stack.

$$V_{act} = -\frac{RT}{2\alpha F} \ln\left(\frac{I_{st}}{S_{cell} J_0}\right) \quad (4)$$

120 Where J_0 is the exchange current density, S_{cell} the active area, I_{st} is the stack current and α is the transfer coefficient.

121

$$V_{conc} = -\frac{RT}{2F} \ln\left(1 - \frac{I_{st}}{I_{max}}\right) \quad (5)$$

122 Where I_{max} is the limit current.

$$V_{ohm} = R_{ohm} I_{st} \quad (6)$$

$$R_{ohm} = R_{mem} + R_c \quad (7)$$

123 Where R_{ohm} is the ohmic resistance which presents the membrane resistance R_{mem} and the contact resistance between
 124 different *PEM* fuel cell layers R_c .

125

126 B. Thermal fuel cell model

127 1) Heat generation

128 Basically, there are four sources of heat generation within *PEM* fuel cell system, which are the entropy change of
 129 reactions, the irreversible loss of electrochemical reactions, and heat resulting from both the ohmic resistance and the
 130 water vapor condensation [27][28]. Knowing that the heat produced by entropy change, irreversible loss and ohmic
 131 resistance is comparable to the fuel cell power output, they present around 55%, 35% and 10% of the total produced
 132 heat, respectively [29]. Indeed, heat generation gives rise to temperature variation within the fuel cell. Therefore, heat
 133 evacuation is considered as a key part to ensure an optimal performance of the fuel cell.

134 Thus, the cooling phenomenon is necessary in order to insure a powerful and efficient fuel cell operation and to
 135 improve the lifetime of the different components. There are three types of cooling methods which are air cooling, liquid
 136 cooling and cooling through phase change [30]. Yet, the air cooling method is the most used widely in applications
 137 with a nominal power less than 5KW insuring the same time a minimum *BOP*, while liquid cooling is used to evacuate
 138 waste heat on high power *PEM* fuel cell greater than 5KW [31] and finally phase change cooling is employed for the
 139 enthalpy of vaporization to evacuate waste heat from the fuel cell [30]. It should be noticed that the cooling through
 140 phase change is benefits compared to conventional liquid cooling [32].

141 Generally, produced heat within the fuel cell is evacuated by two transfer modes. The first one is the natural and forced
 142 convection. In fact, the stack is exposed to the ambient air for this reason it can be cooled by natural convection.

143 Furthermore, in cathode side, the heat removal from the stack is achieved due to fans which explain forced convection
 144 within the stack. The second mode is the conduction which ensures the heat transfer between different layers of fuel
 145 cell. However, heat transfer by forced convection within fuel cell is the most efficient mode [33] because the great part
 146 of generated heat is removed by this transfer mode [21].

147 The generated heat or the dissipated losses in the stack is given by the equation (8)

$$P_e = (N E_{Nernst} - V_{st}) I_{st} \quad (8)$$

148 This equation (8) proves that the generated heat and the fuel cell current vary proportionally. Since, the heat generation
 149 increase is caused by the increase of the stack current, it results also a decrease in the fuel cell voltage. This explains
 150 why the heat generation is more significant at high current demand. Namely, that the high current densities cause a low
 151 system efficiency [34]. Therefore, produced heat should be eliminated from the *PEM* fuel cell system.

152

153 2) Temperature variation

154 Fuel cell operating temperature is considered as a critical parameter since its variation influences the performance and
 155 the efficiency of *PEM* fuel cell [24][35]. On one hand, temperature increase boosts the reaction kinetics and increases
 156 the fuel cell gas diffusivity hence generating a gradual improvement of fuel cell performance at the start up step [23]
 157 [36]. On the other hand, temperature increase beyond a value fixed by the manufacturer causes the fuel cell
 158 performance decrease, since it causes a decrease on membrane conductivity and an increase of membrane resistance.
 159 Also, it engenders a decrease in both relative humidity and water content which results on membrane dehydration [36]
 160 as well as a decrease in the output power of fuel cell system [30]. Therefore, the temperature within the fuel cell needs
 161 to be controlled and the amount of heat produced within the fuel cell must be absolutely eliminated in order to avoid
 162 overheating of the different fuel cell layers which are considered as the critical fuel cell components since their
 163 degradation causes performance loss [37].

164 Thus, a temperature control strategy is essential to limit the performance degradation and improve the *PEM* fuel cell
 165 lifetime. Therefore a fuel thermal model is needed to supervise the temperature variation within the stack.

166 Firstly, the used fuel cell for this study is an open cathode *PEM* fuel cell. Thus the thermal management and the air
 167 supply are ensured by a single actuator piloted by dual axial fans. Consequently, the breakdown of the temperature
 168 control and reactant supply is not evident, therefore, it is necessary to found good compromises between these two
 169 concepts. For this reason, the air supply equation and the thermal equation which takes into account the different losses
 170 sources and heat evacuation modes are considered, in order to design the open cathode *PEM* fuel cell thermal behavior.

171 Equation (9) presents the airflow Q_{air} demanded (given en $L \text{ min}^{-1}$) by the electrochemical reaction tacking place inside
 172 the stack to generate load current.

$$Q_{air} = 60000 \frac{5 N R}{4 P_a F} T_{st} I_{st} S_c \quad (9)$$

173 Where T_{st} is the stack temperature and S_c is the air stoichiometric coefficient, it can be know from equation (9) that the
 174 airflow variation depends on the stack temperature, the stack current and the air stoichiometric coefficient.
 175 Consequently, there is a strong coupling between these parameters.

176 Knowing that, the airflow affects the stack temperature, indeed, it is critical parameters which have an influence on the
 177 fuel cell performance. On one hand, if the supplied airflow is lower than the demanded airflow for cooling purpose the
 178 stack temperature increases. In this case, the airflow lack can cause electrolyte membrane degradation. On the other
 179 hand, an excess airflow reduces the average stack temperature, which leads to a chemical reaction rate decrease. In
 180 addition, this excess airflow creates an overall humidify decrease and the membrane dehydration, thereafter a proton

181 conductivity decrease. Thus, it is evident that the airflow control is an important process to ensure the optimal
182 performance of an open cathode *PEM* fuel cell [38].

183 Assuming that the generated heat within fuel cell is removed by three mechanisms. The first one is the natural
184 convection P_{nat} which is explained by the fact that the fuel cell system is exposed to ambient air, so, heat will be
185 removed from the fuel cell surface to the external environment. The removal heat by natural convection can be
186 expressed as [39]:

$$P_{nat} = h S_{eq} (T_{st} - T_{amb}) \quad (10)$$

187 Where h is the natural convection coefficient, S_{eq} is the equivalent exchange surface.

188 The second one is the forced convection in the cathode side ensured by the axial fans P_{fan} which is defined as following
189 [39].

$$P_{fan} = \frac{1}{60} \rho_{air} Q_{air} C_{p,air} (T_{st} - T_{amb}) \quad (11)$$

190 Where ρ_{air} is the air density, $C_{p,air}$ is the air specific heat.

191 The third mechanism is heat dissipation by phase change liquid/gaseous of water produced inside the *PEM* fuel cell
192 which is expressed by the following equation [39].

$$P_{l/g} = \sigma_{H_2O} \frac{N R}{4 P_a F} T_{st} L_{H_2O} I_{st} k_w \quad (12)$$

193 Where σ_{H_2O} is the water volume density, L_{H_2O} is the latent heat of evaporation of water, k_w is an empirical coefficient
194 representing the water rate produced in liquid forms and then evaporated.

195 Based on energy conservation, the open cathode *PEM* fuel cell thermal equation which describes the heat dissipation
196 mode is given as following:

$$\frac{dT_{st}}{dt} = \frac{1}{m C_{fc}} [\Delta P - P_{nat} - P_{fan} - P_{l/g}] \quad (13)$$

197 Where m is the fuel cell mass, C_{fc} is the fuel cell specific heat.

198 On the right hand side, the first is the source term ΔP which presents the overall rate of generated heat minus the rate of
199 the evacuated heat by the natural convection, the forced convection and the phase change of produced water.

200 All previous equations which describe the fuel cell thermal domain prove that temperature variation within the stack
201 depends on generated heat, flow rate of cooling air and also the specific heat value. Hence, under the same heat flux the
202 stack temperature T_{st} is slowly rising, as the specific heat value is higher [23].

203 *C. proposed model*

204 In order to design an appropriate control strategy, fine and precise fuel cell model is necessary. First of all, the fuel cell
205 is a multi-physic system which requires a coupling between electrical and thermal domain. Indeed, the electric and
206 thermal models are strongly coupled. In fact, through the electrical model, it is possible to determine the fuel cell
207 polarization curve, and to calculate fuel cell and accessory losses. These losses are taken into account to estimate the
208 stack temperature variation through the thermal model.

209 Thus, the proposed model is a combined model which couples electrical and thermal fuel cell models. It is developed in
210 order to reproduce the dynamic behaviour of fuel cells with respect to operating conditions variation. This new custom
211 component implemented in Matlab/Simscape, includes all equations presented above, in the same block.

212 Matlab/Simscape is multi-domain toolbox which is based on an acausal approach. This approach is considered as a
213 relevant approach for this kind type of modeling. Since, it allows assembling several different models such as electrical,
214 thermal, mechanical and aging domain in the same model.

215 The Simscape choice as toolbox to develop our model is justified by the fact that the physical system description does
216 not imply a system behaviour linearization, as with to the Laplace transform or state equations. Consequently, this kind
217 type of toolbox offers the possibility of not being limited to linear systems, further it enables to create physical models
218 which are more in accordance with reality [40]. It should be noticed that the fuel cell proposed model required a
219 coupling between electrical and thermal model which reveals different time scales. Generally, the fuel cell electrical
220 model has a time constant on the order of few seconds, whereas thermal model is extended to a few minutes.

221 The proposed model has as output both the stack temperature T_{st} and the losses inside fuel cell, as an input the fan
222 voltage V_{fan} and an electrical port to allow its integration with other devices in the same application model such as static
223 converters, loads and sources/storages components. Therefore, this proposed model is built to supervise and to control
224 the temperature variation within fuel cell through the fan voltage input, also to test control strategies performance.

225 (The Simscape code of the multi-physic model is given on TABLE II in the APENNDIX 1)

226

227

III. EXPERIMENTAL ESTIMATION OF THE MODEL PARAMETERS

228 The experiment described below was to study the identification of different parameters of the model in order to use
229 them later in the proposed control strategy, which supervises the air stoichiometric ratio and the stack temperature.

230 A. Test bench

231 For experimental validation of the proposed model « *MP_FC* », a commercial open cathode *PEM* fuel cell is used. The
232 installed test bench is composed of an *H-2000* open cathode *PEM* fuel cell, from Horizon technologies. This open
233 cathode *PEM* fuel cell system is self humidified and air cooled stack. It is composed of 48 cells in series. According to
234 the manufacturer's datasheet, the voltage range is 22-48V, the maximum current is 90A and the maximum operating
235 temperature is fixed at 65 °C. It contains two axial fans to ensure simultaneously air supply and air cooling functions.
236 These two fans were powered by an external 12V battery. The maximum fan voltage is about 12V. This stack is
237 embedded with one thermocouple to obtain the temperature variation inside the fuel cell system in real time.

238 Fig.2 presents the schematic of the open cathode *PEM* fuel cell system used for experimental tests.

239

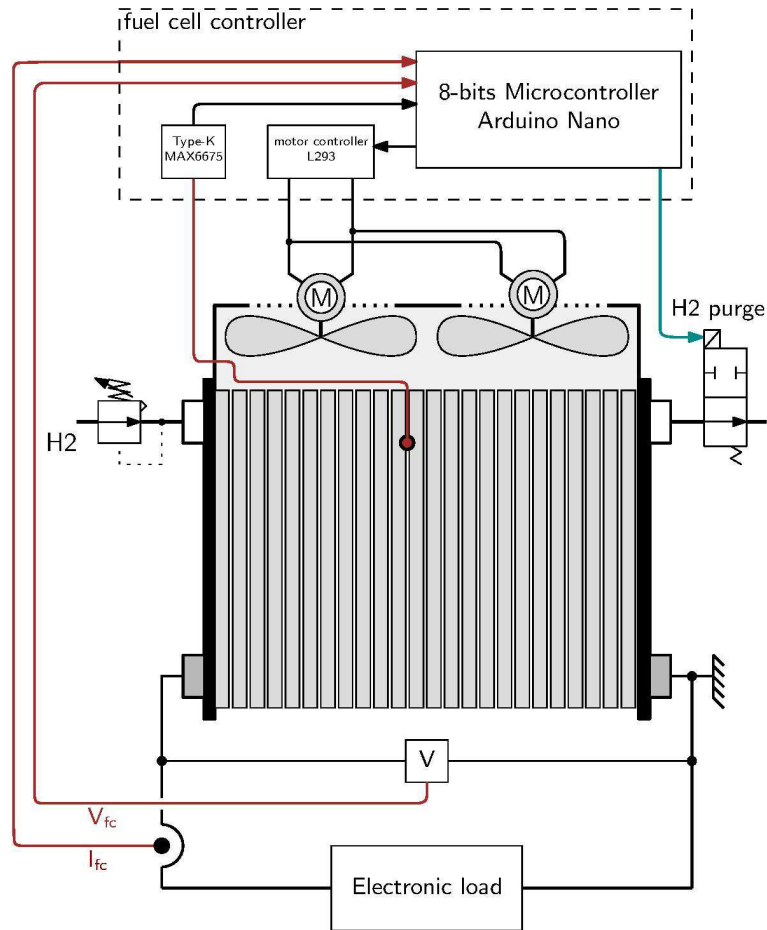


Fig.2. Schematic diagram of the H-2000W open cathode PEM fuel cell system with accessories

240

241

242

243 In addition the test bench includes a programmable load and an acquisition cart that consists of an analog circuit for
 244 voltage temperature and current sensing, associated with an Arduino Nano microcontroller.

245 B. Validation of the electric model of the PEM fuel cell

246 In order to validate the fuel cell electric model, experimental measurements in static mode were carried out.
 247 Experimental tests were conducted for different stack current and with the ancillary controller of the manufacturer.

248 With the equations (1) to (7), a reduced set of parameters must be chosen to make the model close to these
 249 experimental data. Here, we can only consider fitting the transfer coefficient α , the exchange current density J_0 and the
 250 total resistance R_{ohm} . Fig.3 shows the fuel cell polarization curve, obtained from the experimental static measurements
 251 and compared to results generated by model. The comparison between experimental data and simulation results shows
 252 that the electrical fuel cell proposed model follows the characteristics of *H-2000* with acceptable error ranges. It can be
 253 seen that such a simple model is accurate enough to faithfully reproduce the electrical behavior of the fuel cell.

254

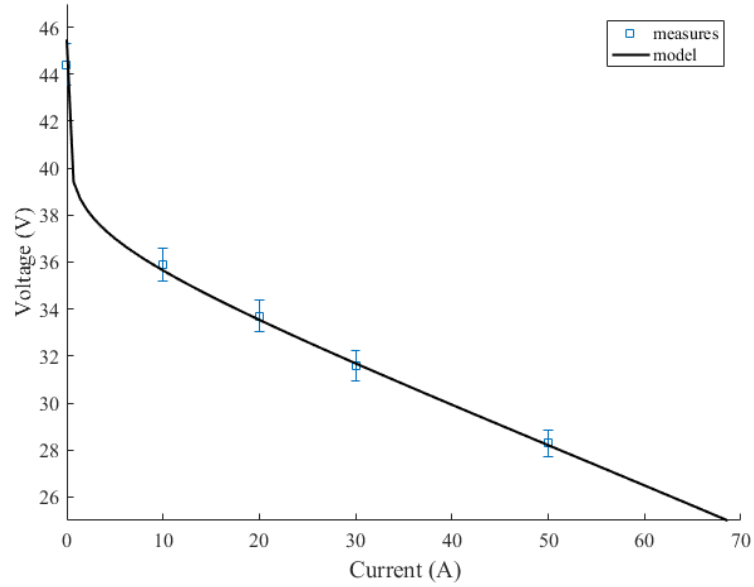


Fig.3. Polarization curve of the used fuel cell

255
256
257

258 C. Validation of the thermal model of the PEM fuel cell and fan characterisation

259 In order to validate the thermal model developed above, both experimental profiles of stack current I_{st} and fan voltage
260 V_{fan} tests were established. During the experimental tests, different fuel cell currents have been imposed and a constant
261 fan voltage has been applied, in order to maintain a stack temperature T_{st} in the range of the rated values (between 40
262 and 65 °C).

263 At thermal balance ($\frac{dT_{st}}{dt} = 0$), the relation between the airflow rate Q_{air} and the fans voltage V_{fan} can be defined from
264 the previous measurements and by knowing these parameters: the electric losses P_e , the stack current I_{st} , the stack
265 temperature T_{st} , and the forced convection term. For this analysis, a measurement error is considered of +/- 2 degrees on
266 the stack temperatures and +/- 25% on the evaporation terms of and natural convection. The identification results
267 obtained are given in Fig.4. As expected maximum operating voltage is 12V and below the value of 2.0V, the fans do
268 not produce any airflow.

269 The empirical relationship obtained by regression is:

270

$$271 \quad Q_{pair}(V_{fan}) = 600 \sqrt{V_{fan} - 2.0} \quad (14)$$

272

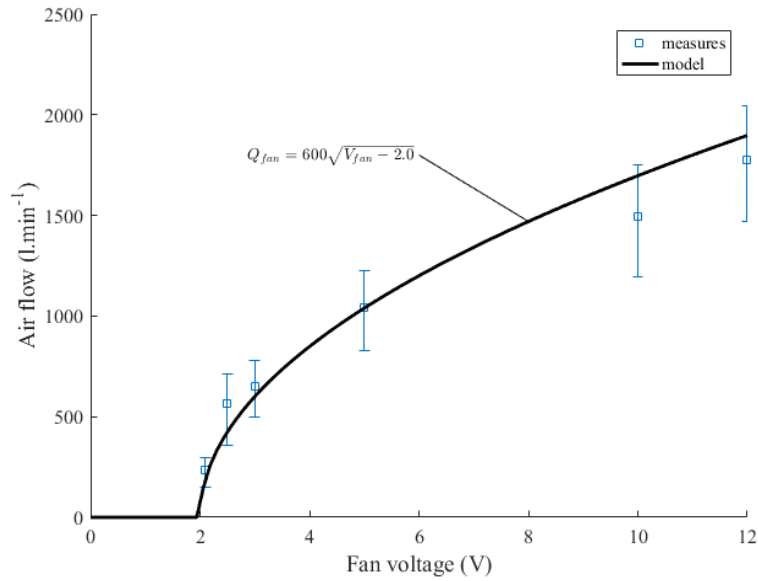


Fig.4. Relation between airflow and the fan voltage

273
274
275

276 Finally, considering the dynamical behavior of thermal model, the mass m and the equivalent specific heat capacity C_{fc}
277 have to be identified. The fuel cell mass is given by the manufacturer. The equivalent specific heat capacity C_{fc} is
278 identified experimentally from measured dynamic responses. Comparison between the model and the experimental
279 measures is done for a current step and by keeping the fan voltage V_{fan} constant (see Fig.5).

280 The thermal model shows an acceptable error in its static and dynamic parts. It can be noted that the model take into
281 account the large time constant of the temperature conditioner, which is about 10 seconds. Finally, the position of
282 temperature sensor inside the stack has a quite high influence on the measurement, because of a non uniform
283 temperature distribution, itself due to the insufficient heat conduction from the core to the edge of stack [23] . For this
284 reason, the temperature sensor is placed as close as possible to the hot spot, which seems to be at the center of the stack.

285
286

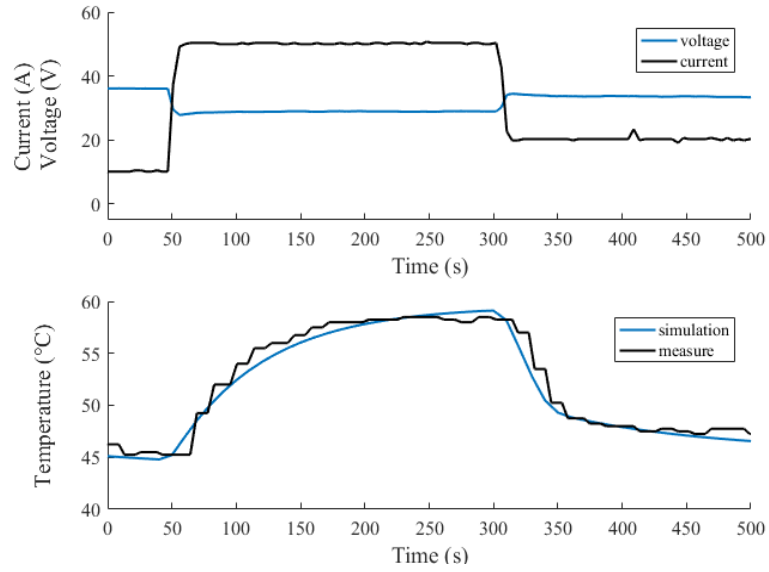


Fig.5. Dynamic response of the fuel cell system, with a constant fan voltage ($V_{fan}=12V$).

Subsequent to experimental and simulation results of the developed electrical and thermal model, similarities between both studies were depicted. As a conclusion, the custom model emulates the *PEM* fuel cell dynamic behaviour.

IV. CONTROL STRATEGY

The control strategy designed in this study is based on the stack temperature regulation and the air stoichiometry adjustment while supplying the needed power. To succeed this objective, the thermal balance equation and the operating constraints applied especially on the stack temperature and the fan voltage are considered in order to design an optimal and safety operation area.

1) Thermal balance study

The open cathode *PEM* fuel cell thermal equation (13) can be studied at thermal balance, which gives the following equation:

$$\Delta P - \sigma_{H_2O} \frac{N R}{4 P_a F} T_{st} L_{H_2O} I_{st} k_w - \frac{1}{60} \rho_{air} Q_{pair} C_{pair} (T_{st} - T_{amb}) - h S_{eq} (T_{st} - T_{amb}) = 0 \quad (15)$$

As mentioned above, the main two parameters that must be controlled during the fuel cell operation are the stack temperature T_{st} and the air stoichiometry coefficient S_c in order to improve the fuel cell performance and efficiency. However, in the case of an open cathode *PEM* fuel cell, these two parameters are strongly coupled. For this reason, there are basically two approaches based on either the operating temperature control [17] or the air stoichiometry adjustment [18] to succeed the stack performance improvement and maximize its efficiency.

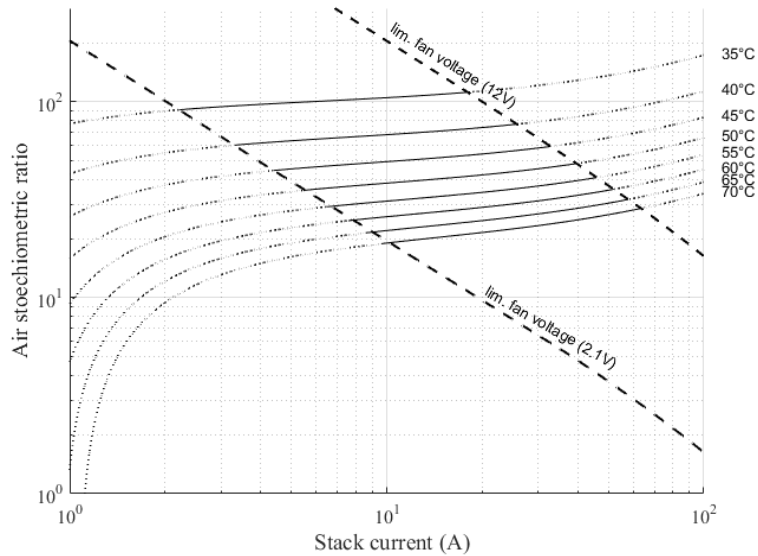
That's why; a functional analysis of equation (15) is done as a first step. Then a robust control strategy is deduced especially in the case of unstable operation.

As a reminder, the problem is governed by 3 main parameters strongly coupled to each other. These parameters are the stack temperature T_{st} , the stack current I_{st} and the air stoichiometric ratio S_c which is directly regulated by the fan

313 voltage. In this context, it is appropriate to add operating constraints particularly applied on the stack temperature and
 314 on the fan operating voltage. These constraints are presented in the equation (16).
 315 The following set of equations (16) is obtained by combining both the thermal balance equation (15) and the airflow
 316 equation (9):

$$317 \left\{ \begin{array}{l} \Delta P - \sigma_{H_2O} \frac{NR}{4 P_a F} T_{st} L_{H_2O} i_{cell} k_w - \rho_{air} \left(1000 \frac{5 NR}{4 P_a F} I_{st} S_c C_{pair} T_{st} \right) (T_{st} - T_{amb}) - h S_{eq} (T_{st} - T_{amb}) = 0 \\ T_{st}^{min} < T_{st} < T_{st}^{max} \\ V_{fan}^{min} < V_{fan} < V_{fan}^{max} \end{array} \right. \quad (16)$$

318 The stack temperature is limited commonly between two values which are T_{st}^{min} around 30-35 °C and T_{st}^{max}
 319 around 65-70°C, also the fans voltage V_{fan}^{max} is limited by the nominal value given by the manufacturer and for V_{fan}^{min} it
 320 should be noted that the various electrical losses and mechanical stress prohibit to fall below 10-20% of the nominal
 321 voltage. Hence, according to the previous equation (16), all the iso-temperature curves $\{I_{st}; S_c\}$ can be drawn. This
 322 result is given in Fig.6 by considering only the stack temperature between 35 and 70°C, and the fan voltage between a
 323 little more than 2V and 12V. It can be observed from these results that the fuel cell controllable zone is situated between
 324 2 and 60A. It is crucial to constantly remember that respecting these defined intervals guarantee a safety operating zone
 325 for the stack since its proper operation is very linked to these parameters. At the top, above the defined controllable
 326 zone the temperature constraint cannot be respected, since the fan voltage limit is exceeded. Besides, below this zone
 327 fan is not sensitive and accurate enough to control the airflow properly.
 328



329
 330 *Fig.6. Synthesis of the static operating points of the used Open cathode PEM fuel cell.*
 331 *The ambient temperature is 25 °C*

333 Taking into account the different operating constraints, an experimental part is done in order to specify stoichiometric
 334 ratio ranges for various current values, which lead the studied system to operate in optimal operating zone. These results
 335 are illustrated in Fig.7. The red dashed lines are the experimental values obtained with a performance decrease less than
 336 2% compared to the optimal solution.

337 As results of this experimental study, an operating zone appeared where a stable and efficient operation is ensured.

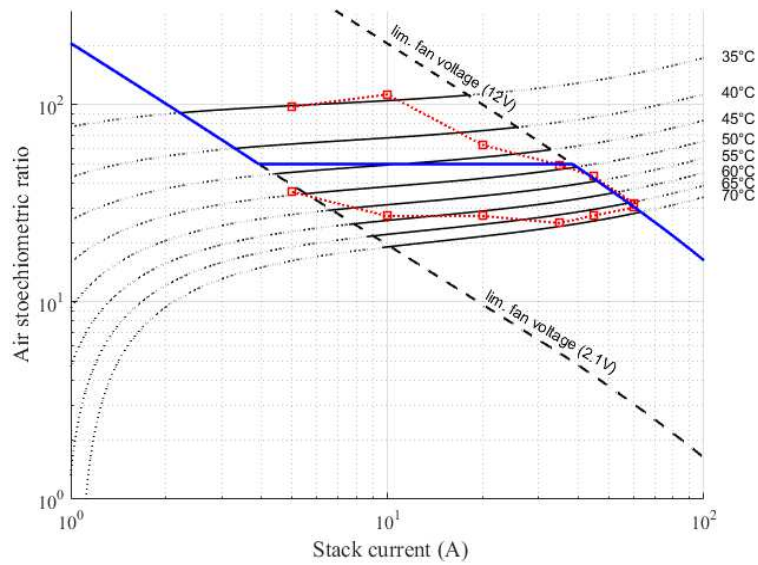


Fig.7. The obtained reference area defining the fuel cell optimal operating zone

339
 340
 341
 342 The main result that can be retired from this configuration is the simple control function, which ensures the studied
 343 system to operate in the safety and optimal operating zone. This latter is a constant stoichiometric ratio, limited by the
 344 operating fan voltage range (2 and 12V), at standard operating conditions (ambient temperature 25 °C), the
 345 stoichiometric coefficient is around 40. Thus, for fan control, it is just sufficient to measure the stack temperature T_{st}
 346 and the stack current I_{st} , to apply them directly in equation (9), then the fan voltage is deduced from the equation (14).
 347 With such control strategy, the temperature is not taken into account and it will be depend on environmental conditions
 348 such as the ambient temperature and the fuel cell performance, which can change significantly over time (reversible and
 349 irreversible damage). Therefore, an over-stoichiometry is added to the control strategy in order to insure the stack
 350 maximum temperature control in transitional or steady state.
 351 To achieve this step, the natural temperature curve in Fig.8 , imposed by the constant stoichiometry control strategy is
 352 considered. It seems that for two different stoichiometric values surrounding the optimum value of $S_C= 40$, the
 353 temperature variation is especially high. Thus, this correlation imposes a secondary temperature control. In order to
 354 ensure system robustness, an average trajectory is chosen.

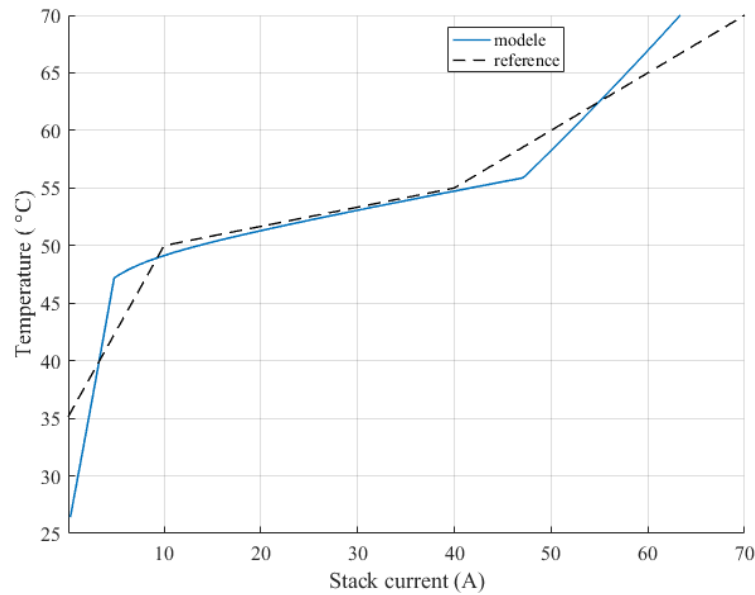


Fig.8. Fuel cell temperature in steady state, for different value of stack current and stoichiometric coefficient

2) Control architecture and implementation

As mentioned in the previous section, the main goal of the proposed control strategy is to define an optimal and safety operating zone for an open cathode *PEM* fuel cell by considering concurrently two criterion, which are the stack temperature regulation and the air stoichiometric adjustment. *Fig.9* shows the control architecture adopted to succeed the goal achievement, which is composed of two paths. The first one considers the calculation of the airflow rate that respects the stoichiometric ratio Sc . The second path calculates the airflow correction to achieve a proper stack temperature. It can be noticed that the temperature regulation can only acts by over stoichiometric action, i.e by increasing the airflow rate, which permits to avoid air starvation. Then, this controller try to find the best balance between both operating temperature and air stoichiometric coefficient with the aim of improving the stack performance.

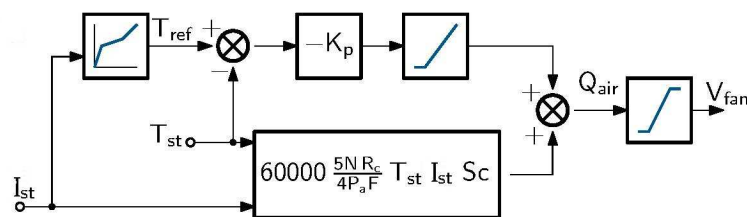


Fig.9. Control architecture for the temperature regulation and air stoichiometric adjustment

In order to evaluate the control strategy performance, simulations are carried out using the same current profile used above. The proposed control strategy integrated with the developed open cathode *PEM* fuel cell model is implemented in Matlab/Simulink environment in *Fig.10*. It can be seen that our developed model of the fuel cell system is easy to be integrated with various components from different library, allowing the proposed control strategy evaluation.

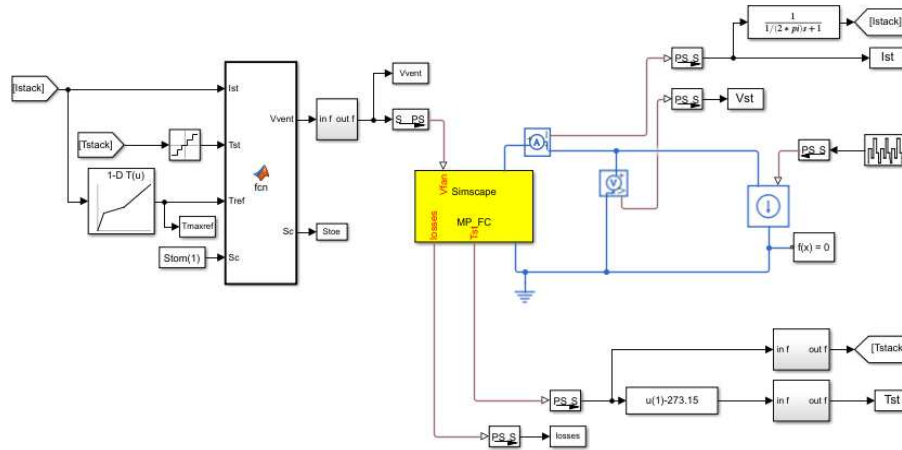


Fig.10. Model implementation in Malab/simulink

As a summary, the proposed work can be divided into the following steps:

1. Identification of both thermal and electrical parameters of the studied system from experimental results (TABLE I),
2. Identification of both fan characteristic curve and fan empirical equation (Fig.4),
3. Definition of controllable zone based an thermal analysis in static mode and operating constraints consideration (Fig.6),
4. Specification of the optimal air stoichiometric curve with respect to the electric characterization of the fan (Fig.7),
5. Integration of an over stoichiometric loop in order to ensure a safety thermal operation,
6. Achievement of experimental and simulation studies and discussion (Fig.12).

3) Results and discussions

Previously mentioned, on one hand the airflow Q_{air} and the cooling fan voltage V_{fan} are strongly linked. On the other hand, the airflow Q_{air} generated to ensure air supply and air cooling depends on these three parameters, the stack current I_{st} , the stack temperature T_{st} and the air stoichiometric coefficient S_C , respectively. In this section, an analysis of the mutual independence between those parameters is carried out.

The measured stack temperature T_{st} , air stoichiometry, fan voltage V_{fan} and stack voltage V_{st} across different stack current values I_{st} are compared with experimental data taken at different air stoichiometric coefficient value 20, 30, 40, 50 respectively. The considered sets of current values are 0, 30, 10, 50, 20, and then 0 A respectively. The ambient temperature is about 25 °C. The fan voltage V_{fan} is varied between 2.1 and 12V. The air stoichiometry is varied between 30 and 150.

Fig.11 shows in red colour the experimental results obtained for several stoichiometric coefficients, 30, 40, and 50 respectively. These results appeared in the optimal operating area defined in the previous section.

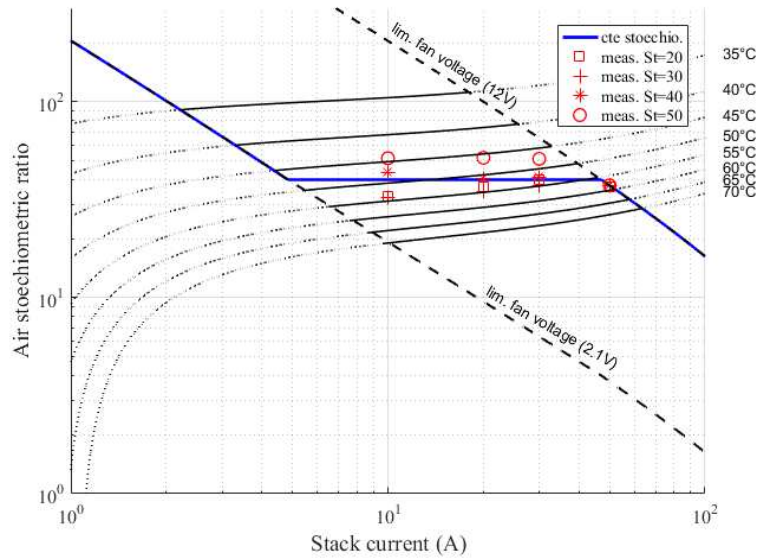


Fig.11. Experimental results implementation in the obtained diagram

a) Fan voltage and fuel cell temperature

As shown in Fig.12, it can be seen that both the fan voltage V_{fan} and the stack temperature variation T_{st} over time depend on current value I_{st} . So, an increase in the stack current leads to an increase in the stack temperature which requires the fan intervention and vice versa.

Since the stack current I_{st} increase, the fan voltage V_{fan} increase to insure simultaneously both air supply for electrochemical reaction taking place inside the stack and the temperature regulation by generated heat evacuation allowing the temperature decrease within the fuel cell system. Accordingly, a high value of fan voltage V_{fan} is needed because of the temperature increase resulting from heat generation. Subsequently, the fan voltage value V_{fan} is relatively low due to the lower stack temperature value. In order to confirm this concept taking the example, at $I_{st} = 50$ A and $S_C = 30$, it can be seen that the temperature increase from 49 °C to reach 60 °C at that moment the fan acts to supply air and evacuated heat in order to decrease temperature that should not exceed a reference value. In this case, the fan voltage attains its maximum value which is 12V. While, for the same value of stoichiometric coefficient S_C and $I_{st} = 20$ A, it can be notice that the stack temperature reaches a smaller value compared to this reached at $I_{st} = 50$ A. Moreover, the fan voltage is about 3V.

b) Fan voltage and stoichiometric coefficient

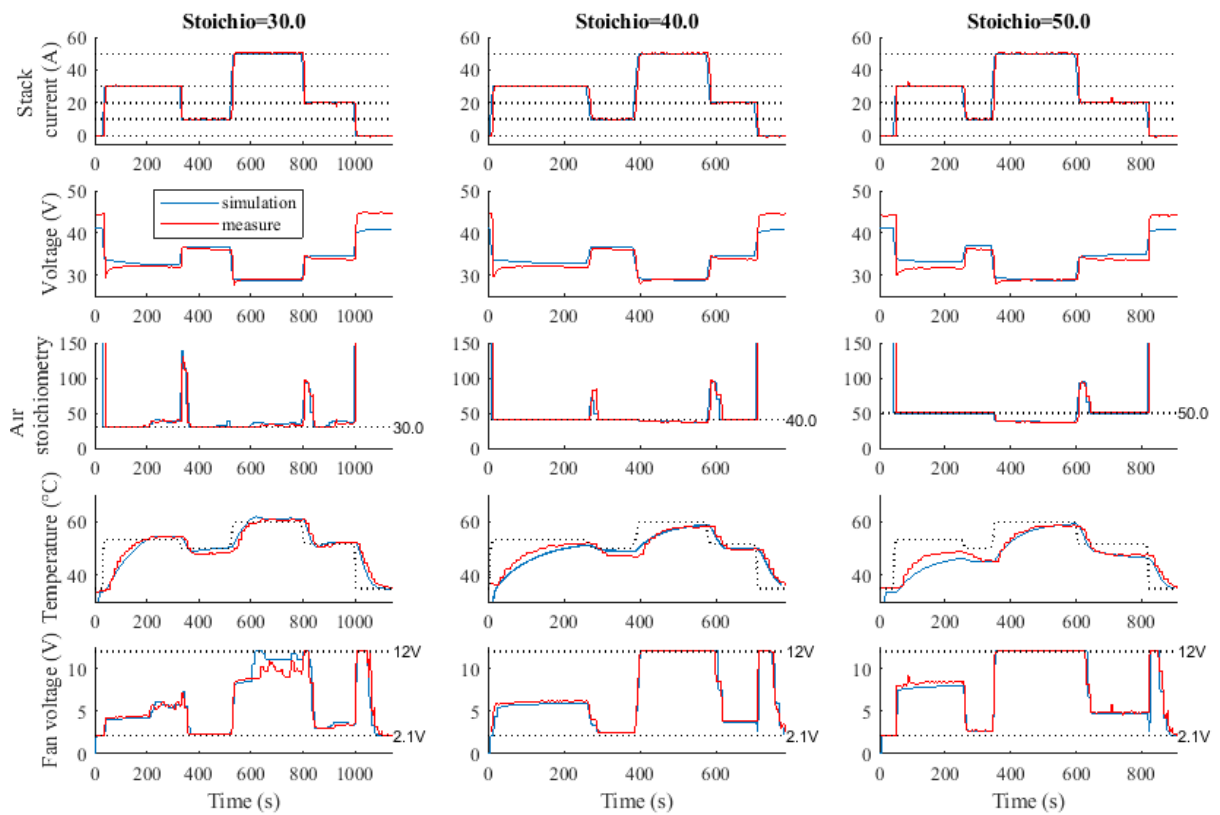
The fan voltage V_{fan} is proportional to the stack current I_{st} , the stack temperature T_{st} and the stoichiometric coefficient S_C . Fig.12 shows an increase in stoichiometric coefficient S_C leads to an increase on the fan voltage V_{fan} . So, high value of stoichiometric coefficient S_C relatively requires a high fan voltage V_{fan} in order to provide the demanded airflow. For example at $S_C = 30$ and $I_{st} = 20$ A, the fan voltage is about 3.2V, yet, at $S_C = 50$ and by keeping the same stack current value ($I_{st} = 20$ A) the fan voltage V_{fan} is more greater, it reaches a value of about 4.8V. Consequently, for the first considered case the fuel cell temperature is about 52.7 °C, since the fuel cell temperature in the second case is lower and attains 47.75 °C. Indeed, at high stoichiometric coefficient S_C , there is an excess of supplying air within the fuel cell which contribute to improve the cooling process of the stack.

429 c) Fan voltage and stack current

430 Based on Fig.12, it can be noticed the strong relation between the stack current I_{st} and the fan voltage V_{fan} . In fact, the
 431 increase in the stack current I_{st} engenders an increase the stack temperature T_{st} , which demands the fan voltage V_{fan}
 432 increase, simply to ensure both the air supply and the fuel cell cooling. For example at $I_{st} = 20$ A and $S_C = 30$, the fan
 433 voltage is about 3.2V, yet, at $I_{st} = 50$ A and by keeping the same stoichiometric value ($S_C = 20$ A) the fan voltage V_{fan} is
 434 more important, it reaches its maximum value which is 12 V, in the same time, it prevent the stack temperature T_{st} to
 435 exceed the reference value.

436 Previous analysis, explains the strong coupling between the stack current I_{st} , the stack temperature T_{st} , the air
 437 stoichiometric coefficient S_C and the fan voltage V_{fan} . As a conclusion, there is a good agreement between simulations
 438 results and experimental data of the proposed control strategy which confirm subsequently its efficiency.

439



440

441 *Fig.12. Comparison between the simulation results and the experimental data*

442 Parameters of the used open cathode PEM fuel cell are given in Erreur ! Source du renvoi introuvable..

443

444

445

446

447

448

449

450

TABLE I FUEL CELL PARAMETERS

Description	Symbol	Value	Unit
Oxygen pressure	PO ₂	0.5	Bar
Hydrogen pressure	PH ₂	0.5	Bar
Reversible single cell potential	E ₀	1.2	V
Exchange current	J ₀	4e-7	A/m ²
Active cell area	Scell	100e-4	m ²
Limit current	I _{max}	90	A
Molar gas constant	R	8.3144	J/(mol.K)
Faraday constant	F	9648	J/(mol.V)
Ohmic resistance	Rohm	2.9	mΩ
Number of elementary cell	N	48	–
Mass	m	10	kg
Air density	rho	1.2	kg/m ³
Fuel cell specific heat	C _p	3000	J/(kg.K)
Air specific heat	C _{p-air}	1000	J/(kg.K)
latent heat of water steam	LH ₂₀	2500	kJ.kg ⁻¹
Liquid to steam coefficient	kw	0.3	
Atmospheric pressure	P _a	101 300	Pa
Natural convection coefficient	h	3	W.K ⁻¹ .m ⁻²
Equivalent surface of natural convection	S _{eq}	0.15	m ²
Proportional controller gain	K _p	250	V. K ⁻¹

452

453

V. CONCLUSION

454 The main goal of this work is to design an appropriate control strategy which combining simultaneously the stack
 455 temperature regulation and the air stoichiometry adjustment in order to guarantee the performance improvement and the
 456 degradation prevention of the studied system. To succeed on designing this control strategy with respect to operating
 457 conditions change, an accurate model of fuel cell system is necessary. A multi-physical model is developed in
 458 MATLAB/Simscape based on acausal modeling approach. It allows mainly emulating the dynamic behaviour of an
 459 open cathode fuel cell system under different operating conditions and controlling stack temperature through the fan
 460 voltage input. An experimental part by using 2 kW open cathode fuel cell gives validation of the proposed model. The
 461 main innovative aspect of the developed model is its ease of integration with different components from different
 462 library. Several domains are integrated in the same bloc independently from each other. Another feature of the designed
 463 model is its improvement by inserting more domains in the same bloc already developed, such as ageing domain.

464 Temperature variations in the fuel cell system are considered as a critical factor as its increase beyond a specific value
 465 causes thermal stresses and reduces the system performance and efficiency. As well airflow rate for both supplying and
 466 air cooling tasks is an important factor in an open cathode fuel cell system. Therefore, these two parameters have a
 467 significant role in the fuel cell thermal management.

468 System thermal balance was studied for two issues. The first one is to release the fuel cell fans characterization.
 469 Knowing that, the fan empirical equation is deduced from experimental results. The second one is to find the best
 470 compromise between these two parameters which are the air stoichiometric coefficient S_c and the fuel cell temperature
 471 T_{sc} in order to guarantee an optimal fuel cell performance. Through the proposed control strategy, an optimal and safety
 472 operating zone is defined in which the fuel cell performance is better. This zone is defined as a constant stoichiometric

473 air ratio of 40 surrounded by the operating limit of the fan voltage (2.1 and 12V) and the stack temperature. The
474 comparison between experimental and simulation results prove the effectiveness of the appropriate control strategy with
475 different operating conditions. Consequently, a temperature increase caused by the load current increase requires an
476 excess of supplying air in order to ensure the system cooling and to avoid performance degradation.

477

478

ACKNOWLEDGMENT

479 This work was supported by the Tunisian Ministry of High Education and Research under Grant LSE-ENIT-
480 LR11ES15, and Institute of Research on Electrical Energy of Nantes Atlantique - IREENA, Saint-Nazaire, France.

481

REFERENCES

- 482 [1] G. R. Molaeimanesh, M. A. Bamdezh, and M. Nazemian, "Impact of catalyst layer morphology on the performance of PEM fuel cell cathode
483 via lattice Boltzmann simulation," *Int. J. Hydrogen Energy*, pp. 1–17, 2018.
- 484 [2] M. Andersson, S. B. Beale, M. Espinoza, Z. Wu, and W. Lehnert, "A review of cell-scale multiphase flow modeling , including water
485 management , in polymer electrolyte fuel cells," *Appl. Energy*, vol. 180, pp. 757–778, 2016.
- 486 [3] J. Han, S. Yu, and S. Yi, "Advanced thermal management of automotive fuel cells using a model reference adaptive control algorithm," *Int. J.*
487 *Hydrogen Energy*, vol. 42, no. 7, pp. 4328–4341, 2016.
- 488 [4] S. Slouma, S. Skander Mustapha1, I. Slama Belkhodja1, M. Orab, "An improved simple Fuel Cell model for Energy Management in residential
489 buildings" , *J. Electrical Systems*, vol. 11, pp. 145_159, 2015.
- 490 [5] S. L. Chavan and D. B. Talange, "Modeling and performance evaluation of PEM fuel cell by controlling its input parameters," *Energy*, vol. 138,
491 pp. 437–445, 2017.
- 492 [6] G. Zhang and K. Jiao, "Multi-phase models for water and thermal management of proton exchange membrane fuel cell : A review," *J. Power*
493 *Sources*, vol. 391, no. February, pp. 120–133, 2018.
- 494 [7] R. M. Aslam, D. B. Ingham, M. S. Ismail, K. J. Hughes, L. Ma, and M. Pourkashanian, "Simultaneous thermal and visual imaging of liquid
495 water of the PEM fuel cell flow channels," *J. Energy Institute*, pp. 1–8, 2018.
- 496 [8] S. M. Rahgoshay, A. A. Ranjbar, A. Ramiar, and E. Alizadeh, "Thermal investigation of a PEM fuel cell with cooling flow field," *Energy*, vol.
497 134, pp. 61–73, 2017.
- 498 [9] Z. M. Huang, A. Su, C. J. Hsu, and Y. C. Liu, "A high-efficiency, compact design of open-cathode type PEMFCs with a hydrogen generation
499 system," *Fuel*, vol. 122, pp. 76–81, 2014.
- 500 [10] J. C. Olivier , G. Wasselynck, D. Trichet, N. Bernard, S. Hmam, S. Chevalier, C. Josset, B. Auvity, G. Squadrito, "Multiphysics Modeling and
501 Driving Strategy Optimization of an Urban-Concept Vehicle," 2015 IEEE Veh. Power Propuls. Conf. VPPC 2015 - Proc., 2015.
- 502 [11] J. Ishaku, N. Lotfi, H. Zomorodi, and R. G. Landers, "Control-oriented modeling for open-cathode fuel cell systems," *Proc. Am. Control Conf.*,
503 pp. 268–273, 2014.
- 504 [12] K. Latha, S. Vidhya, B. Umamaheswari, N. Rajalakshmi, and K. S. Dhathathreyan, "Tuning of PEM fuel cell model parameters for prediction
505 of steady state and dynamic performance under various operating conditions," *Int. J. Hydrogen Energy*, vol. 38, no. 5, pp. 2370–2386, 2013.
- 506 [13] Y. Tang, W. Yuan, M. Pan, Z. Li, G. Chen, and Y. Li, "Experimental investigation of dynamic performance and transient responses of a kW-
507 class PEM fuel cell stack under various load changes," *Appl. Energy*, vol. 87, no. 4, pp. 1410–1417, 2010.
- 508 [14] Q. Li, W. Chen, S. Liu, Z. Gao, and S. Yang, "Temperature optimization and control of optimal performance for a 300W open cathode proton
509 exchange membrane fuel cell," *Procedia Eng.*, vol. 29, pp. 179–183, 2012.
- 510 [15] R. Costa-Castelló and S. Strahl, "Model-based analysis for the thermal management of open-cathode proton exchange membrane fuel cell
511 systems concerning efficiency and stability," *J. Process Control*, vol. 47, pp. 201–212, 2016.
- 512 [16] W. Binrui, J. Yinglian, X. Hong, and W. Ling, "Temperature control of PEM fuel cell stack application on robot using fuzzy incremental PID,"
513 *Control Decis. Conf. CCDC'09. Chinese*, pp. 3293–3297, 2009.
- 514 [17] S. Strahl, A. Husar, P. Puleston, and J. Riera, "Performance improvement by temperature control of an open-cathode PEM fuel cell system,"
515 *Fuel Cells*, vol. 14, no. 3, pp. 466–478, 2014.

- 516 [18] F. Buaud, D. Lelandais, and B. Auvity, "Evidence of a non-dimensional parameter controlling the flooding of PEMFC stack," *Int. J. Hydrogen*
517 *Energy*, vol. 33, no. 11, pp. 2765–2773, 2008.
- 518 [19] K. Ou, W. W. Yuan, M. Choi, S. Yang, and Y. B. Kim, "Performance increase for an open-cathode PEM fuel cell with humidity and
519 temperature control," *Int. J. Hydrogen Energy*, vol. 42, no. 50, pp. 29852–29862, 2017.
- 520 [20] K. Ou, Y. Wang, and Y. Kim, "Performance Optimization for Open- cathode Fuel Cell Systems with Overheating Protection and Air Starvation
521 Prevention," *Fuel Cells*, no. 3, pp. 299–307, 2017.
- 522 [21] Q. Jian, B. Huang, L. Luo, J. Zhao, S. Cao, and Z. Huang, "Experimental investigation of the thermal response of open-cathode proton
523 exchange membrane fuel cell stack," *Int. J. Hydrogen Energy*, vol. 3, 2018.
- 524 [22] M. R. Islam, B. Shabani, G. Rosengarten, and J. Andrews, "The potential of using nanofluids in PEM fuel cell cooling systems: A review,"
525 *Renew. Sustain. Energy Rev.*, vol. 48, pp. 523–539, 2015.
- 526 [23] Y. Tang, W. Yuan, M. Pan, Z. Li, G. Chen, and Y. Li, "Experimental investigation of dynamic performance and transient responses of a kW-
527 class PEM fuel cell stack under various load changes," *Appl. Energy*, vol. 87, no. 4, pp. 1410–1417, 2010.
- 528 [24] Q. Li, W. Chen, S. Liu, Z. Gao, and S. Yang, "Temperature optimization and control of optimal performance for a 300W open cathode proton
529 exchange membrane fuel cell," *Procedia Eng.*, vol. 29, pp. 179–183, 2012.
- 530 [25] S. Slouma, S. Skander Mustapha, I. Slama Belkhdja, M. Orabi, " Simple fuel cell model for stand_alone hybrid system energy management,"
531 *Proc. IEEE International Conference on Modeling and Simulation of Electric Machines, Converters and Systems (ELECTRIMACS)*, May 2014.
- 532 [26] O'Hayre R, Cha S-W, Colella W, Prinz FB. *Fuel cell fundamentals*. 2 ed. New York: John Wiley & Sons; 2009
- 533 [27] H. Ju, H. Meng, and C. Y. Wang, "A single-phase, non-isothermal model for PEM fuel cells," *Int. J. Heat Mass Transf.*, vol. 48, no. 7, pp.
534 1303–1315, 2005.
- 535 [28] Agus P. Sasmito, Erik Birgersson and Arun S. Mujumdar, " Numerical investigation of liguide water cooling for a proton ecchange membrane
536 fuel cell stack", *Heat Transfer Engineering*, vol. 32, pp. 151-167, 2010.
- 537 [29] S.G. Goebel, *Evaporative cooled fuel cell*, US Patent 6,960,404, assigned to General Motors Corporation, 2005.
- 538 [30] A. Fly and R. H. Thring, "A comparison of evaporative and liquid cooling methods for fuel cell vehicles," *Int. J. Hydrogen Energy*, vol. 41, no.
539 32, pp. 14217–14229, 2016.
- 540 [31] A Dicks, DAJ Rand, *fuel cells explained*, wiley online library, 2018
- 541 [32] G. Zhang and S. G. Kandlikar, "A critical review of cooling techniques in proton exchange membrane fuel cell stacks," *Int. J. Hydrogen Energy*,
542 vol. 37, no. 3, pp. 2412–2429, 2012.
- 543 [33] S. Yu and D. Jung, "A study of operation strategy of cooling module with dynamic fuel cell system model for transportation application,"
544 *Renew. Energy*, vol. 35, no. 11, pp. 2525–2532, 2010.
- 545 [34] Hosseinzadeh, M. Rokni, A. Rabbani, and H. H. Mortensen, "Thermal and water management of low temperature Proton Exchange Membrane
546 Fuel Cell in fork-lift truck power system," *Appl. Energy*, vol. 104, pp. 434–444, 2013.
- 547 [35] H. Al-Zeyoudi, A. P. Sasmito, and T. Shamim, "Performance evaluation of an open-cathode PEM fuel cell stack under ambient conditions: Case
548 study of United Arab Emirates," *Energy Convers. Manag.*, vol. 105, pp. 798–809, 2015.
- 549 [36] Q. Yan, H. Toghiani, and H. Causey, "Steady state and dynamic performance of proton exchange membrane fuel cells (PEMFCs) under various
550 operating conditions and load changes," *J. Power Sources*, vol. 161, no. 1, pp. 492–502, 2006.
- 551 [37] L. Placca and R. Kouta, "Fault tree analysis for PEM fuel cell degradation process modelling," *Int. J. Hydrogen Energy*, vol. 36, no. 19, pp.
552 12393–12405, 2011.
- 553 [38] S. Strahl, A. Husar, and J. Riera, "Experimental study of hydrogen purge effects on performance and efficiency of an open-cathode Proton
554 Exchange Membrane fuel cell system," *J. Power Sources*, vol. 248, pp. 474–482, 2014.
- 555 [39] J. C. Olivier, G. Wasselyncq, S. Chevalier, B. Auvity, C. Josset, D. Trichet G. Squadrito, N. Bernard, "Multiphysics modeling and optimization
556 of the driving strategy of a light duty fuel cell vehicle,". *Int. J. Hydrogen Energy*, vol. 42, pp. 26943–26955, 2017.
- 557 [40] S. Hmam, J. C. Olivier, S. Bourguet, and L. Loron, "A Multirate Simulation Method for Large Timescale Systems Applied for Lifetime
558 Simulations," 2015 *IEEE Veh. Power Propuls. Conf. VPPC 2015 - Proc.*, 2015.

559
560
561

TABLE II CODE OF THE MULTI-PHYSIC PEM FUEL CELL MODEL IMPLEMENTED IN MATLAB/SIMSCAPE

```

component MP_FC < foundation.electrical.source %Multi-Physic FC
inputs
    Vvent = {0, 'V'}; %Vfan:top
end
outputs
    Tfc = {0, 'K'}; %Tst:bottom
    Per = {0, 'W'}; %losses:bottom
end
parameters
    PO2 = 0.5; % Pressure of oxygen
    PH2 = 0.5; % Pressure of Hydrogen
    Eo = {1.2, 'V'}; % Reversible single cell potential,
    Io = {6e-7, 'A/m^2'}; % Exchange current
    Sact = {100e-4, 'm^2'}; % Surface active
    Imax = {100, 'A'}; % Limit current
    T = {298.15, 'K'}; % Ambient temperature
    R = {8.3144, 'J/(mol*K)'}; % Molar gas constant
    F = {96485, 'J/(mol*V)'}; % The Faraday's constant
    Alpha = {0.77, '1'}; % Transfer coefficient
    Rohm = {0.0029, 'Ohm'}; % Ohmic resistance
    N = {48, '1'}; % Number of elementary cells
    m = {10, 'kg'}; % Mass
    Cp = {300, 'J/(kg*K)'}; % Specific heat of fuel cell
    Cp_air = {1000, 'J/(kg*K)'}; % Specific heat of air
    rho = {1.2, 'kg/m^3'}; % Air density
    a = {600, 'm^3/(s*V^0.5)'};
    g = {1, 'A'};
    V0 = {2.0, 'V'}; % Minimum fan voltage
    LH2O = {2500e3, 'J*kg^-1'}; % Water latent heat of evaporation
    Pa = {101300, 'kg*m^-1*s^-2'}; % Atmospheric pressure
    rh2o = {1e3, 'kg/m^3'}; % water volume density
    kw = {0.5, '1'}; % Wasselynck coefficient
    h = {3, 'W/m^2/K'}; % Wasselynck coefficient
    Seq = {0.14, 'm^2'}; % Heat exchange surface
end

variables
    ist = {0, 'A'}; % Stack current
    Eth = {0, 'V'}; % Thermodynamic potential
    Vconc = {0, 'V'}; % Concentration losses
    Vohm = {0, 'V'}; % Ohmic losses
    Vact = {0, 'V'}; % Activation losses
    Tst = {0, 'K'}; % Stack temperature
    Qv = {0, 'm^3/s'}; % Coolant flow rate
end
equations
    v == N*(Eth-Vohm-Vact-Vconc); % Stack voltage
    Eth == Eo+(0.5*(R*Tst/F))*(log(PH2)+0.5*log(PO2)); %Reversible voltage
    Vconc == -0.5*(R*Tst/F)*log(1-(ist/Imax)); %Concentration losses
    Vact == (0.5*(R*Tst)/(Alpha*F))*(log(max(ist,g)/(Sact*Io))); %Activation losses
    Vohm == icell*Rohm; %Ohmic losses
    Tst.der==1/(m*Cp)*(Per - (rho*Cp_air*Qv*(Tst-T)) - 1e-3*kw*rh2o*ist*N*R/(4*Pa*F)*Tst*LH2O -
h*Seq*(Tst-T)); %Temperature variation
    Per== N*(Eth-v)* ist; %Dissipated losses
    Qv== a*max(0,(Vvent - V0))^(0.5)/60000; %Qv=f(Vfan)

    ist == -I;
    Tfc == Tst;
end
end

```